Thermodynamics of Wheat Germ Agglutinin-Sialyloligosaccharide Interactions by Proton Nuclear Magnetic Resonance†

K. Anne Kronis‡ and Jeremy P. Carver*

Departments of Medical Genetics and Medical Biophysics, University of Toronto, Toronto, Ontario, Canada M5S 1A8
Received May 2, 1984; Revised Manuscript Received August 28, 1984

ABSTRACT: The thermodynamic parameters that characterize the binding of wheat germ agglutinin isolectin I (WGA I) to the α2-3 isomer of (*N*-acetylneuraminyl)lactose have been determined by 360-MHz proton nuclear magnetic resonance spectroscopy. The chemical exchange of the ligand between the free and bound sites resulted in a broadening and upfield shifting of the *N*-acetyl methyl resonance [Kronis, K. A., & Carver, J. P. (1985) *Biochemistry* (preceding paper in this issue)] which has allowed the determination of the equilibrium constant, K_D, and the dissociation rate constant, k_D. In this paper, the analysis of the temperature dependence of the K_D values between 25.4 and 51.6 °C yielded equilibrium parameters indicative of a large entropy barrier to binding: $\Delta H° = -13.3 \pm 1.0$ kcal mol^{-1} and $\Delta S° = -31.9 \pm 2.4$ cal mol^{-1} K^{-1}. The Arrhenius plot of the effect of temperature on the dissociation rate (k_D) and the plot of ln (k_D/T) vs. $1/T$ indicated that the transition complex represented an unfavorable energy state compared to the dissociated molecules with an activation energy (E_A) of +18.0 kcal mol^{-1} and enthalpy and entropy of dissociation ($\Delta H_D^‡$ and $\Delta S_D^‡$) values of +17.4 ± 0.3 kcal mol^{-1} and +13.4 ± 1.2 cal mol^{-1} K^{-1}, respectively. The driving force for this binding reaction is the large negative $\Delta H°$ with a small enthalpic barrier to association ($\Delta H_A^‡ =$ +4.1 kcal mol^{-1}). In spite of a large enthalpy of binding, the dissociation constants measured for WGA I binding to this sialylated molecule are in the millimolar range, a result that stems directly from the large entropy barriers to the associated complex ($\Delta S°$ and $\Delta S_A^‡ = -31.9$ and -18.5 cal mol^{-1} K^{-1}, respectively). In contrast to the negative entropy observed for this system, hydrophobic or ionic interactions are expected to exhibit positive $\Delta S°$ values. Thus, earlier suggestions [Kabat, E. A., Liao, J., Burzynska, M. H., Wong, T. C., Thorgersen, H., & Lemieux, R. U. (1981) *Mol. Immunol. 18*, 873-881] that hydrophobic interactions are the major contributors to protein-sugar complex formation are in direct contradiction with the results of this study. Rather, the dominant forces stabilizing the associated complex would appear to be intermolecular *hydrogen bonds* and *van der Waals'* forces since negative $\Delta S°$ and $\Delta H°$ values are typical of such interactions [Ross, P. D., & Subramanian, S. (1981) *Biochemistry 20*, 3096-3102].

Lectins are an extensively studied class of proteins that are able to agglutinate cells and/or precipitate glycoconjugates (Goldstein et al., 1980). Since lectin-like molecules, present on the surfaces of cells, are presumed to be important in cell-cell interactions by virtue of their ability to bind to exposed carbohydrates, a molecular characterization of the mechanisms of lectin-sugar interactions will undoubtably aid in our understanding of a wide range of biological processes. The vast majority of lectin binding studies have focused upon the measurement of dissociation constants (K_D's)[1] at one temperature. As with any macromolecule-ligand interaction, the forces that stabilize the bound complex can only be delineated through a careful study of the equilibrium (thermodynamic) and kinetic (activation) parameters. To this end, we have quantified these parameters for the binding of the α2-3 isomer of (*N*-acetylneuraminyl)lactose (N3L) to wheat germ agglutinin isolectin I (WGA I) by high-resolution proton nuclear magnetic resonance (^{1}H NMR) spectroscopy at 360 MHz. Other characteristics of this system are analyzed in the preceding paper (Kronis & Carver, 1985; K. A. Kronis and J. P. Carver, unpublished results).

There exist several opposing views as to what molecular aspects of bound complexes are responsible for their stability. In an analysis of published data, Ross & Subramanian (1981) concluded that the negative values of $\Delta H°$ and $\Delta S°$ observed for many protein-ligand binding reactions are due to hydrogen bonding and van der Walls' attractions.[2] This was an empirical observation that was made by comparing published equilibrium thermodynamic parameters with the respective crystal structures for many protein-protein and protein-ligand complexes. By examining the three-dimensional shapes of certain carbohydrate antigens, Kabat et al. (1981) proposed that the hydrophobic effect drives the nonpolar face of a sugar molecule out of the water and onto the hydrophobic protein

† This research was supported by grants from the National Cancer Institute of Canada and from the Medical Research Council of Canada (MT-3732 and MA-6499). This paper represents part of the Ph.D. thesis work of K.A.K.

* Address correspondence to this author at the Department of Medical Genetics.

‡ Present address: Departments of Chemistry and Biology, Massachusetts Institute of Technology, Cambridge, MA 02139.

[1] Abbreviations: WGA I, wheat germ agglutinin I; PNA, peanut agglutinin; NeuNAc, *N*-acetyl-D-neuraminic acid; N3L, α2-3 isomer of (*N*-acetylneuraminyl)lactose, NeuNAcα2-3Galβ1-4Glc; MUF, 4-methylumbelliferyl; GlcNAc, *N*-acetyl-D-glucosamine; ^{1}H NMR, proton nuclear magnetic resonance; UV, ultraviolet; K_D, dissociation constant; k_D, dissociation rate; k_A, association rate; $\Delta G°$, Gibbs free energy of binding; $\Delta H°$, enthalpy of binding; $\Delta S°$, entropy of binding; $\Delta X_A^‡$ and $\Delta X_D^‡$, activation parameters for association and dissociation, respectively, where X can be H, S, or G; E_A, activation energy of dissociation; Con A, concanavalin A.

[2] The superscript degree symbol has been used to denote equilibrium thermodynamic values such as $\Delta G°$, $\Delta H°$, and $\Delta S°$. Although this superscript should be reserved for values measured at standard conditions, it is commonly used in the above context for data derived from the studies of biological interactions.

0006-2960/85/0424-0834$01.50/0

surface, implying that $\Delta S°$ is positive and enthalpic terms are less important. Janin & Chothia (1978) suggested that hydrophobic forces compensated for the losses in translational and rotational degrees of freedom of a ligand upon binding. In an effort to clarify what factors lend stability to the interaction of a commonly used plant lectin with a cell surface analogue, we have measured the temperature dependence of the K_D value of WGA I for N3L and determined the signs and magnitudes of $\Delta H°$ and $\Delta S°$.

An additional reason for a detailed consideration of this system is that many of the equilibrium thermodynamic parameters that have been published for lectin–sugar interactions have been obtained by using hydrophobically tagged sugars bearing fluorescent, visible, or UV probes. These groups may influence the results because of additional entropic factors that may arise from the portion of the molecule that constitutes the "probe" and not from the sugar moiety for which the lectin is "specific". Furthermore, several lectins such as Con A and lima bean lectin are known to have hydrophobic sites which are removed from the sugar binding site on the protein surface (Hardman & Ainsworth, 1973; Edelman & Wang, 1978; Roberts & Goldstein, 1982). Thus, we have concentrated on a cell-surface analogue of the WGA receptors of mammalian cells, unencumbered with hydrophobic residues.

The activation parameters, $\Delta H^‡$ and $\Delta S^‡$, have rarely been determined for the association or dissociation rates of lectin–ligand reactions due to the absence of kinetic data. Kinetic parameters enable one to examine the energetics of the transition state. In the preceding paper (Kronis & Carver, 1985), the equations of Swift & Connick (1962) were solved for the bound shift and bound lifetime ($\Delta\omega_B$ and τ_M, respectively) of the *N*-acetyl resonance of N3L at various temperatures. The τ_M values have been used in this study to determine the temperature dependence of the dissociation rate, k_D. This has allowed the E_A, $\Delta H_D^‡$, and $\Delta S_D^‡$ values to be assigned for the conversion of the associated complex to its transition state. A model of the energetics of the dissociated, activated, and complexed states has been proposed that is consistent with the thermodynamic parameters reported in this paper. The equilibrium and kinetic parameters thus allow us to describe the forces involved in the formation of, as well as the stabilization of, the WGA I–N3L complex.

Experimental Procedures

Materials. WGA I and N3L were purified, characterized, and prepared for ^1H NMR titrations (Kronis & Carver, 1982, 1985). Deuterated buffer (0.1 M NaP_i–0.15 M NaCl, pD 6.1 ± 0.1) was prepared in 99.96% D_2O (Kronis & Carver, 1982).

NMR Binding Experiments. The titrations involving WGA I and N3L were reported in Kronis & Carver (1985). The $\Delta\omega_{Bapp}$ and $1/T_{2Bapp}$ for several ligand resonances were analyzed in order to determine the bound shifts ($\Delta\omega_B$'s) for those hydrogens using the equations derived by Swift & Connick (1962). The exchange lifetime (τ_M) was determined for the N3L molecule from the Swift–Connick solutions of the *N*-acetyl data [see Kronis & Carver (1985) for the data treatment and the $\Delta\omega_B$ solutions]. In this work, the τ_M values are reported and the temperature dependence of the K_D and k_D values are analyzed. The value of k_D is obtained from the reciprocal of τ_M ($\tau_M = k_D^{-1}$) for the Swift–Connick solutions of the data reported in Kronis & Carver (1985) by using a value of 2 for *n*, the number of binding sites on the WGA I monomer (Kronis & Carver, 1985). The instrumental conditions, the temperature calibration of the titrations, and numerical analyses are as outlined previously (Kronis & Carver, 1985).

Binding Theory. In a simple bimolecular process, a ligand, A, binds to a protein, P, in a dynamic fashion, characterized by a second-order association rate constant, k_A (M^{-1} s^{-1}), and a first-order dissociation rate constant, k_D (s^{-1}), as shown by

$$A + P \underset{k_D}{\overset{k_A}{\rightleftharpoons}} PA \qquad (1)$$

The energy barrier to binding is presumed to be due to an activated transition state, $[PA]^‡$, which is energetically unfavorable:

$$A + P \underset{k_{-A}}{\overset{k_A}{\rightleftharpoons}} [PA]^‡ \underset{k_D}{\overset{k_{-D}}{\rightleftharpoons}} PA \qquad (2)$$

The dissociation constant, K_D (molar), is equal to the ratio of the two rates shown in eq 1 if the concentration of $[PA]^‡$ is small compared with $[A]_F$, $[P]_F$, and [PA], where F denotes the free, as opposed to bound (B), concentration. In other words, if the rate-limiting steps in the reaction scheme, shown in eq 2, are k_A and k_D, by virtue of the unfavorable energetics associated with the transition state, then the K_D is the ratio of these rates:

$$K_D = k_D/k_A \qquad (3)$$

The K_D value is a function of the Gibbs free energy of binding ($\Delta G°$), the enthalpy of binding ($\Delta H°$), and the entropy of binding ($\Delta S°$), as given by

$$\ln (K_D) = \frac{\Delta G°}{RT} = \frac{\Delta H°}{RT} - \frac{\Delta S°}{R} \qquad (4)$$

where R is the gas constant, T is the temperature (K), and $\Delta G°$, $\Delta H°$, and $\Delta S°$ are the thermodynamic constants for the association of the PA complex: i.e., from left to right in the schemes shown in eq 1 and 2.

The effect of temperature on the rate constant, k_D, may be used to determine the activation energy, as well as the activation enthalpy and entropy of dissociation (E_A, $\Delta H_D^‡$, and $\Delta S_D^‡$, respectively), for the reaction. An Arrhenius plot of $\ln (k_D)$ vs. $1/T$ affords a slope of $-E_A/R$ according to eq 5

$$\ln (k_D) = \ln (A) - E_A/(RT) \qquad (5)$$

where A is the frequency factor. Plots of $\ln (k_D/T)$ vs. $1/T$, according to transition state theory, yield $\Delta H_D^‡$ and $\Delta S_D^‡$:

$$\ln (k_D/T) = \frac{-\Delta H_D^‡}{RT} + \frac{\Delta S_D^‡}{R} + \frac{k}{h} \qquad (6)$$

where k and h are the Boltzmann and Plank constants, respectively.

Results

Temperature Dependence of the Dissociation Constant for N3L Binding to WGA I. In the presence of WGA I, the *N*-acetyl resonance of the NeuNAc residue of N3L is broadened and shifted to higher field due to chemical exchange of the sugar between the bound environment at the protein binding site and the free environment in solution (Kronis & Carver, 1982, 1985). The change in line width ($\Delta\Delta\nu$, in Hz) and the change in chemical shift ($\Delta\delta$, in Hz) are both proportional to X_B, the fraction of ligand, A, that is bound to the protein ($X_B = [A]_B/[A]_T$) [see Kronis & Carver (1982, 1985)]. Thus, these alterations in the ligand resonance may be used to determine equilibrium dissociation constants, K_D's (molar). When the experiments are performed as a function of temperature, the variation in K_D's can be analyzed to give the equilibrium thermodynamic parameters, $\Delta H°$ and $\Delta S°$. In addition, the NMR experiment yields an estimate of the dissociation rate for the protein–ligand complex, and from the

Table I: Dissociation Constants (K_D's) and Gibbs' Free Energies ($\Delta G°$'s) Determined at Various Temperatures for N3L Binding to WGA I

	$-\Delta\delta$[b]		$\Delta\Delta\nu$[c]		
T[a] (°C)	K_D (mM)	c.c.	K_D (mM)	c.c.	$\Delta G°$[d] (kcal mol^{-1})
25	–		1.0	av	–, –4.1
31.5	2.3	0.95	4.1	0.996	–3.7, –3.3
37.8	3.9	0.99	4.8	0.997	–3.4, –3.3
42.0	5.7	0.995	6.7	0.99	–3.2, –3.1
47.3	7.4	0.99	8.2	0.99	–3.1, –3.1
51.6	10.3	0.97	–		–3.0, –

[a] The temperature T (°C) was calibrated from the chemical shift of the HDO resonance (Kronis & Carver, 1985). [b] The K_D values shown in this column were obtained from the absolute value of the y intercept of plots of $[A]_T$ (mM) vs. $-\Delta\delta^{-1}$ (Hz^{-1}), where $-\Delta\delta$ is the magnitude of the upfield shift of the N-acetyl resonance. The correlation coefficient (c.c.) of the fit is indicated. [c] The K_D values in this column were similarly obtained from the negative y intercept of plots of $[A]_T$ (mM) vs. $\Delta\Delta\nu^{-1}$ (Hz^{-1}), where $\Delta\Delta\nu$ is the lifetime broadening of the N-acetyl resonance and c.c. represents the correlation coefficient. The K_D at 25 °C represents the average (av) of seven experiments at 25 ± 1 °C. [d] The $\Delta G°$ values were computed for the corresponding values by using $\Delta G° = RT \ln (K_D)$, where R is the gas constant (1.99 cal mol^{-1} K^{-1}) and T is the temperature (K). The two values listed represent the $\Delta G°$ values derived from the plots of $[A]_T$ vs. $-\Delta\delta^{-1}$ and $\Delta\Delta\nu^{-1}$, respectively.

temperature dependence of this rate the activation parameters (E_A, $\Delta H^‡$, and $\Delta S^‡$) can be determined.

The NMR data for the N-acetyl singlet peak were the most suitable, of the three peaks monitored in Kronis & Carver (1985), for accurate K_D measurements. The resulting values are reported in Table I together with the corresponding $\Delta G°$ values. Also included are the results of several additional experiments, including one titration at 51.6 °C in which the shifting of the N-acetyl resonance was used to determine the K_D, as well as the average K_D and $\Delta G°$ values for seven room temperature experiments. The first column of K_D values and the first $\Delta G°$ value at any temperature correspond to those obtained by using $-\Delta\delta$ data in the form of $[A]_T$ vs. $-\Delta\delta^{-1}$ plots (Kronis & Carver, 1985). The second column and set of $\Delta G°$ values were derived from $[A]_T$ vs. $\Delta\Delta\nu^{-1}$ plots.

The individual fits of the data, described above, all had high correlation coefficients (Table I). The scatter or range of values found when comparing K_D's at one temperature from the shifting and/or the broadening data is rather large compared with the scatter of the individual fits. A comparison of data, collected over several years, indicates that there is an additional fluctuation in the K_D values, resulting in a fluctuation in $\Delta G°$ values measured at one temperature, of approximately ±0.2 kcal mol^{-1}, that we have ascribed to variations in unknown instrumental parameters that change with time. It is apparent from the data in Table I that, for a given temperature, this range is sufficient to account for the variations in the affinities. If one restricts the analysis to one shifted parameter or carries out the experiments over a short period (weeks), then the free energy range at a particular temperature can be reduced to ±0.1 kcal mol^{-1} (Kronis & Carver, 1982), and relative differences of this magnitude can be detected with confidence. However, because of the larger long-term variations, the *absolute* value of any given $\Delta G°$ has to be considered to have a ±0.4 kcal mol^{-1} error associated with its value.

The temperature dependence of the equilibrium dissociation constant may be used to determine $\Delta H°$ and $\Delta S°$ from a van't Hoff plot of ln (K_D) vs. $1/T$ as shown in Figure 1 for the data summarized in Table I. The errors in the slopes and intercepts were estimated from the dotted lines shown in Figure 1, between which all the data are included. The slope of the line

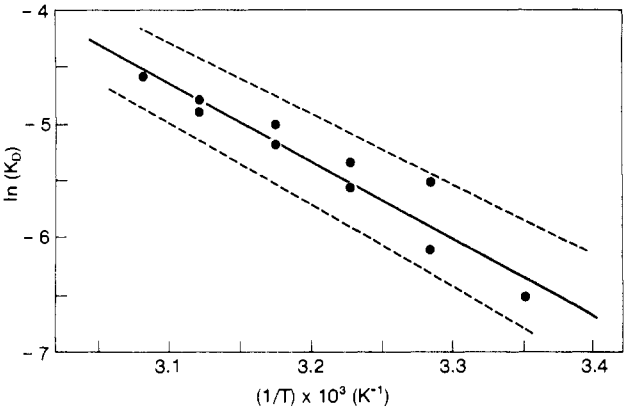

FIGURE 1: van't Hoff plot of the binding of N3L to WGA I. The dissociation constants, reported in Table I, are plotted as ln (K_D) vs. $1/T$. The dashed lines represent estimates on the error in the fits and were used to estimate the errors in the resulting $\Delta H°$ and $\Delta S°$ values obtained from the slope and intercept of this plot, respectively.

Table II: Summary of the Thermodynamic Parameters for N3L–WGA I[a]

parameter (units)	equilibrium ($\Delta X°$)	activation dissociation ($\Delta X_D^‡$)	activation association ($\Delta X_A^‡$)
ΔH (kcal mol^{-1})	–13.3 ± 1.0	+17.4 ± 0.3	+4.1
ΔS (cal mol^{-1} K^{-1})	–31.9 ± 2.4	+13.4 ± 1.2	–18.5
$-T\Delta S$ (kcal mol^{-1})	+9.5 ± 0.7	–4.0 ± 0.4	+5.5
ΔG (kcal mol^{-1})	–3.8 ± 0.4	+13.4 ± 0.7	+9.6

data from Arrhenius plot: E_A = +18.0 kcal mol^{-1}; $A = 1.5 \times 10^{16}$

[a] The X refers to one of H, S, or G for the appropriate enthalpy, entropy, or free energy. The equilibrium parameters were derived from plots such as is shown in Figure 1. The results of different experiments afforded equilibrium parameters in the range quoted in this table. The errors were obtained as described in the text. The activation dissociation values were derived from plots such as Figure 2. The errors were determined as described in the text. For comparison $T\Delta S$ values have been calculated for 298 K. The activation association values were calculated by using $\Delta X_A^‡ = \Delta X° + \Delta X_D^‡$. No errors are quoted on these values since there was no independent determination of k_A values in this system. The ΔG values have been calculated by using $\Delta G = \Delta H - T\Delta S$ (298 K), and the errors were determined as described in the text.

afforded a $\Delta H°$ of –13.3 ± 1.0 kcal mol^{-1}. The entropy of binding, $\Delta S°$, was found to be –31.9 ± 2.4 cal mol^{-1} K^{-1} from the y intercept. These values are listed in Table II, along with the other parameters that characterize the binding (see below).

Temperature Dependence of the Dissociation Rate of the N3L–WGA I Complex. In our previous study (Kronis & Carver, 1985), the apparent bound line width and the apparent bound shift values of the N-acetyl peak for a given temperature were solved by using the equations of Swift & Connick (1962). The Swift–Connick solutions yield the bound shift, ($\Delta\omega_B$), the transverse relaxation time in the bound site (T_{2B}), and the lifetime of the resonance in the bound state (τ_M). The T_{2B} values were not found to be a significant factor in the solutions of the apparent bound expressions, and the solutions were consistent with a potential range of T_{2B} values of (1.2–2.0) $\times 10^{-2}$ s. In this section, we analyse the temperature dependence of τ_M, calculated from the N-acetyl data assuming that the two binding sites per monomer have equivalent bound lifetimes [see Kronis & Carver (1985)].

In order to be detectable in an NMR binding experiment in which one is monitoring the lifetime shifting or broadening of a ligand resonance, a binding site must be characterized by a different ligand chemical shift (ω) and/or T_2 value than that experienced in the absence of protein. The τ_M value, obtained from such an NMR experiment, corresponds to the

Table III: Dissociation Rates (k_D's) and Their τ_M Values[a]

T (K)	$\tau_M \times 10^4$ (s)	k_D range $\times 10^{-3}$ (s^{-1})	ln (k_D/T)
298.4	9.68 ± 0.50	0.98–1.09	1.24 ± 0.05
304.5	5.85 ± 0.45	1.59–1.85	1.73 ± 0.08
309.8	3.30 ± 0.26	2.81–3.29	2.28 ± 0.08
315.0	2.03 ± 0.23	4.42–5.56	2.76 ± 0.11
320.3	1.27 ± 0.17	6.94–9.09	3.21 ± 0.14

[a] The τ_M values for one experiment represent the Swift–Connick solutions described in Kronis & Carver (1985). The k_D ranges were computed by using $\tau_M = k_D^{-1}$ for the range of τ_M values and were used to calculate a range of ln (k_D/T) values for each temperature. The value was taken as the average of the extremes, and the error includes the range of values.

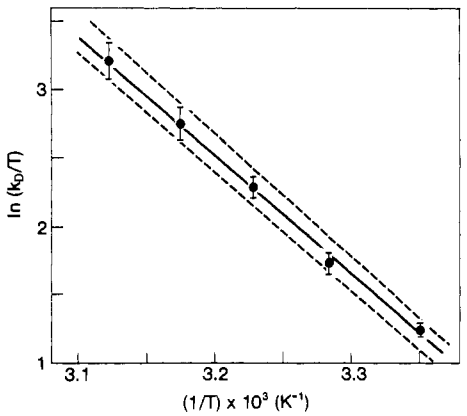

FIGURE 2: Temperature dependence of the dissociation rate. The k_D values (Table III) have been plotted as ln (k_D/T) vs. $1/T$. The errors in the k_D and ln (k_D/T) values were determined from the errors in the τ_M values used to compute them as described in the text and summarized in Table III. The dashed lines represent the errors in the fit used in the determination of the ΔH_D^* and ΔS_D^* and their errors.

average lifetime spent by the ligand in the binding site. Thus, the dissociation rate of N3L calculated from τ_M ($\tau_M = k_D^{-1}$) is that of the rate-limiting step in the transition from the complex (ω_B, T_{2B}) to the free state (ω_F, T_{2F}). For simplicity's sake we will refer to this dissociation rate as k_D (see eq 1 and 2) and will discuss its location in the binding reaction path later (see Discussion).

The expression $\tau_M = k_D^{-1}$ was used to calculate the k_D values (Table III) corresponding to the τ_M solutions of the binding data reported in Kronis & Carver (1985). The values of k_D show the typical exponential relationship with temperature expected for a first-order rate constant. The activation energy (E_A) for this process was determined to be +18.0 kcal mol^{-1} from an Arrhenius plot of ln (k_D) vs. $1/T$ (Table II). The frequency factor, A, is also listed in Table II.

Alternatively, the data may be analyzed according to transition-state theory which allows the calculation of the enthalpy of activation (ΔH_D^*), and the entropy of activation (ΔS_D^*) for the dissociation of the bound complex to the transition state at a rate k_D. The activation free energy, at a particular temperature, may then be calculated by using $\Delta G_D^* = \Delta H_D^* - T\Delta S_D^*$. The data for one experiment are plotted as ln (k_D/T) vs. $1/T$ in Figure 2, and the resulting activation parameters for dissociation are summarized in Table II. The errors in the τ_M values were used to determine errors in k_D values by calculating the range of k_D's that corresponded to the range of τ_M values (Table III). The k_D was taken as the mean of the k_D range of values, while the errors in Figure 2 correspond to that range. The errors in the slopes and intercepts, used to determine the errors in ΔH_D^* and ΔS_D^*, were estimated from the range of values that correspond to

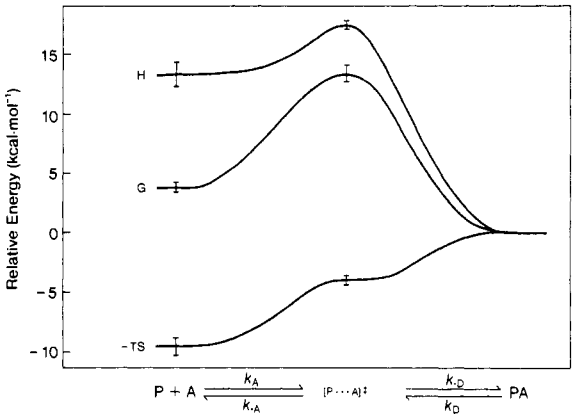

FIGURE 3: Energy profile for the binding reaction. The relative energy levels of the thermodynamic parameters have been plotted vs. the proposed reaction path. The labels for the curves are H, for the enthalpy levels, G for the free energy levels and $-TS$ for the entropy, calculated for a temperature (T) of 298 K. The binding scheme is depicted along the x axis. The relative energy of the bound complex has been taken to be of zero energy so that higher energy level states have positive relative energies in this figure.

the dashed lines in Figure 2, as was done for the equilibrium data. The ΔH_D^* and ΔS_D^* values determined for the dissociation of N3L from the WGA I molecule (as monitored by τ_M) were +17.4 ± 0.3 kcal mol^{-1} and +13.4 ± 1.2 cal mol^{-1} K^{-1}, respectively. At 298 K, the ΔG_D^* value would be +13.4 kcal mol^{-1}, indicative of a highly unfavorable state. These values, along with the equilibrium values, will be compared below to results from other lectin–sugar binding studies (see Discussion).

Energy Level Scheme for the Binding of N3L to WGA I. The equilibrium and kinetic thermodynamic parameters reported in this study for the WGA I binding of N3L are represented schematically in Figure 3 for a temperature of 298 K. The *relative* energy levels of the portions of the binding scheme have been computed by setting the bound complex (PA) at 0 kcal mol^{-1}. Entropy is represented by $-TS$, enthalpy by H, and free energy (calculated by using the appropriate ΔH and $T\Delta S$ values) as G.

The overall $\Delta H°$ value (−13.3 ± 1.0 kcal mol^{-1}; Table II), corresponds to the difference between the dissociated molecules and the complex. Similarly $-T\Delta S°$ (+9.5 ± 0.7 kcal mol^{-1} at 298 K) is this difference on the $-TS$ curve. The $\Delta G°$ value for association is the sum of these $\Delta H°$ and $-T\Delta S°$ values and corresponds to −3.8 kcal mol^{-1}. The error in the G curve for the dissociated state (±0.4 kcal mol^{-1}) represents the absolute error in $\Delta G°$ values obtained from $\Delta G° = RT \ln K_D$ for many experiments performed at approximately 298 K (25 ± 1 °C) over a period of several years.

The relative enthalpy and entropy energy levels of the transition state have been determined from the effect of temperature on the dissociation rate (Figure 2; Tables II and III). The errors on the H and $-TS$ curves for the activated complex were obtained from the errors of fits such as Figure 2. This afforded a ΔH_D^* value of +17.4 ± 0.3 kcal mol^{-1} and a $-T\Delta S_D^*$ value of −4.0 ± 0.4 kcal mol^{-1} at 298 K. The free energy level for this activated state was computed from the sum of these two values and from the sum of their largest errors: $\Delta G_D^* = +13.4 \pm 0.7$ kcal mol^{-1}. Independent estimates of the error on ΔG_D^*, calculated from the errors in k_D values at 298 K, were within this range.

Finally, the kinetic association parameters were obtained from the sum of the overall equilibrium and dissociation activation energy values (Table II): $\Delta H_A^* = +4.1$ kcal mol^{-1}; $\Delta S_A^* = -18.5$ cal mol^{-1}; $-T\Delta S_A^* = +5.5$ kcal mol^{-1} (at 298

Table IV: Thermodynamic Parameters for Lectin–Sugar Interactions

thermodynamic parameter	value (kcal mol^{-1}) from reference[a]		
	1	2	3
$\Delta G°$	−3.8	−5.9	−4.3
$\Delta H°$	−13.3	−8.2	−16.8
$-T\Delta S°$	+9.5	+2.3	+12.4
ΔG_D^*	+13.4		+15.4
ΔH_D^*	+17.4		+13.4
$-T\Delta S_D^*$	−4.0		+2.0
ΔG_A^*	+9.6		+11.1
ΔH_A^*	+4.1		−3.5
$-T\Delta S_A^*$	+5.5		+14.6

[a] The references are the following: 1, this work; 2, Van Landschoot et al. (1977); 3, Neurohr et al. (1982). The lectins and ligands used in these studies were WGA I and N3L (1), WGA and MUF–GlcNAc (2), and PNA and β-methyllactose (3).

K); ΔG_A^* = +9.6 kcal mol^{-1} (at 298 K) (see Discussion). Thus, there is an overall energy barrier to binding characterized by a positive ΔG_A^*, due to a small enthalpic barrier of +4.1 kcal mol^{-1} and a larger entropic barrier ($-T\Delta S_A^*$ of +5.5 kcal mol^{-1} at 298 K). The energy gained by proceeding from the activated complex to the bound state is large. The free energy of −13.4 kcal mol^{-1} for $-\Delta G_D^*$ comes from a large enthalpic gain in energy ($-\Delta H_D^*$ = −17.4 kcal mol^{-1}) with an additional entropy penalty for association ($+T\Delta S_D^*$ = +4.0 kcal mol^{-1} at 298 K).

Discussion

Affinity of WGA I for N3L Decreases with Increasing Temperature. The temperature dependence of the K_D for the interaction of WGA I with N3L indicated that the affinity decreased as the temperature increased. This is not the result of a denaturation process or an unfolding of the protein structure since WGA is stable to heat and denaturing agents (Rice & Etzler, 1975; Marchesi, 1972). The stability of the protein presumably results from the 16 interdomain disulfide bonds per monomer (Rice & Etzler, 1975; Wright, 1977). The data obtained at 51.6 °C gave results consistent with the data obtained at other temperatures (Table I; Figure 1), and furthermore, the samples that had been used to conduct titrations above 45 °C gave the predicted spectrum when analyzed subsequently at 25 °C [see Kronis & Carver (1985)]. Further evidence in support of the stability of the protein conformation over this temperature range comes from the invariance of the bound site geometry, as reflected in the bound shift values ($\Delta\omega_B$'s) for three resonances of the NeuNAc portion of N3L (Kronis & Carver, 1985). These $\Delta\omega_B$ values represent the bound orientation of the corresponding hydrogens relative to aromatic amino acid side chains. For these reasons, we are confident that the observed decrease in affinity with temperature is solely the result of the energetics of the binding.

Van Landschoot et al. (1977), in a study of the binding of MUF-substituted GlcNAc oligomers with WGA, also reported values of $\Delta H°$ and $\Delta S°$ (see Table IV). In that study, the affinities were also shown to decrease with increasing temperature. This observation is not likely to be solely due to the presence of the MUF substituent since a large decrease in affinity with increasing temperature was found for several GlcNAc-containing oligomers by Lacelle (1979) by using ^{1}H NMR and extrinsic fluorescence competition methods. In contrast Privat et al. (1974), monitoring intrinsic protein fluorescence, detected only a very slight decrease in affinity of WGA for GlcNAcβ1–4GlcNAcβ1–4GlcNAc from 6 to 50 °C. However, this latter result may arise from the inherent problems in correcting the fluorescence data for the effects of temperature.

Characteristics of the Activated State in the Binding Scheme. The rate-limiting steps in the proposed binding scheme (see eq 2 and Figure 3) were assumed to be k_A and k_D for the association and dissociation of the complex, respectively. This is valid, as long as the concentration of the $[PA]^*$ species is small compared with those of the dissociated molecules and the bound complexes. By use of the value obtained for the activation energy for dissociation (E_A), the Boltzmann distribution of molecules between the activated and associated states was found to be 8×10^{-14}, indicating that the assumption of a short-lived activated complex was valid.

The parameter τ_M in the Swift–Connick equations is proportional to the half-life of a ligand in a site, characterized by the bound shifts and bound relaxation times (ω_B and T_{2B}, respectively), compared to a state in which these parameters are those of the free ligand. The rate-limiting step in the dissociation of the complex is the formation of the transition state, and hence, τ_M can be used to determine k_D in eq 2 and Figure 3. However, the chemical shift of the *N*-acetyl of N3L in the *transition* state cannot be determined, since it is the overall chemical shift difference between the bound and free environments that is monitored.

Signs and Magnitudes of the Equilibrium and Activation Enthalpies: Hydrogen Bonds and van der Waals' Forces Stabilize the Complex. It is of interest to compare the magnitude of $\Delta H°$ with the interactions identified in the crystal complexes. Several hydrogen bonds have been postulated on the basis of the distances between potential donors and acceptors in the S_{BC} site[3] (Wright, 1980a,b): four hydrogen bonds seemed likely with the possibility of one or two more which were less defined. Also, several van der Waals' contacts have been predicted from the data derived on the NeuNAc- and N3L–WGA II crystal complexes at site S_{BC} (Wright, 1980a,b). Empirically, it has been found that hydrogen bonds and van der Waals' forces contribute to the enthalpy of the bound complex (Ross & Subramanian, 1981). If we assume that the enthalpic contribution made by hydrogen bonds and van der Walls' forces arises in the conversion of the transition state to the complex (Ross & Subramanian, 1981), then the ΔH_D^* value of +17.4 ± 0.3 kcal mol^{-1} is a quantitative measure of that contribution. Thus, the observed ΔH_D^* value would correspond to a maximum of −2.9 to −4.3 kcal mol^{-1} for the average enthalpic contribution of each of the four to six proposed hydrogen bonds and somewhat less energy if van der Waals' interactions are significant. This range is reasonable for hydrogen bond strengths (Barker, 1971). The small enthalpy barrier to the formation of the activated complex, +4.1 kcal mol^{-1}, could represent the heat of removal of bound water molecules from the site and possibly from the ligand.

Signs and Magnitudes of the Equilibrium and Activation Entropies: The Bound Complex Is Entropically Disfavored. The equilibrium entropy of association was found to be quite large in this system, corresponding to a $-T\Delta S°$ value of +9.5 ± 0.7 kcal mol^{-1} at 298 K, which represents roughly 70% of the energy that is gained in enthalpy upon binding. Thus, the large entropy barrier to association can be concluded to be the cause of the millimolar affinities that have been measured for the binding of N3L to WGA (Kronis & Carver, 1982, 1985). For example, a 50% reduction in the entropy barrier would

[3] The sugar binding sites of WGA are named as described in Kronis & Carver (1985): the site at the interface of the B and C domains is S_{BC} while that at the interface of the A and D domains is S_{AD}.

yield a $\Delta G°$ of −8.5 kcal mol^{-1} and a K_D of less than 1 μM. A similarly large entropy barrier was found for β-methyllactose binding to peanut agglutinin (PNA) resulting once again in a millimolar K_D (Neurohr et al., 1982; Table IV). In contrast, concanavalin A exhibits a similar $\Delta H°$ for a branched trimannoside but a smaller entropy barrier (A. E. MacKenzie and J. P. Carver, unpublished results), thus yielding a 100-fold tighter saccharide binding than was observed for WGA or PNA.

The increase in affinity often observed when hydrophobic tags are added to saccharide ligands may arise from a reduction in the entropic barrier to complex formation and not necessarily from additional enthalpic interactions with the protein (Das et al., 1979). As an example, the affinity of MUF–GlcNAc for WGA (Van Landschoot et al., 1977) is higher than that for N3L, and as is shown in Table IV, this increase in affinity arises from a significant decrease in the entropy barrier for the labeled ligand. A qualitatively similar result was observed with MUF–NeuNAc (Kronis, 1983) compared to that of NeuNAc (Jordan et al., 1977) or N3L (Kronis & Carver, 1982, 1985; this work). Thus, at least in these cases, the increased affinity arises from the reduced entropy barrier which, in turn, likely stems from the lower entropy of the hydrophobically modified ligand in the *free* state.

Models for the Origin of the Entropy Barrier. The activation entropy for association $\Delta S_A^‡$, computed as the sum of $\Delta S°$ and $\Delta S_D^‡$, was approximately half the equilibrium value (Table IV). Thus, the overall entropy barrier is made up of two entropically unfavored steps in the binding scheme shown in Figure 3. Two different mechanisms have been proposed to account for the transition from the *dissociated* molecules to this *activated* state (Ross & Subramanian, 1981). If the activated state represents a partially immobilized complex, then the $-\Delta S_A^‡$ value will be positive, due to the loss of the six translational and rotational degrees of freedom (Janin & Chothia, 1978; Ross & Subramanian, 1981). An alternate process of association, resulting from hydrophobic interactions, predicts negative $-\Delta S_A^‡$ values (Ross & Subramanian, 1981). The data reported in this study, along with the data obtained for the association of β-methyllactose with PNA (Neurohr et al., 1982; Table IV), are consistent with the former case in which formation of the associated state is entropically disfavored.

Although the association of N3L with WGA and β-methyllactose with PNA are characterized by similar thermodynamic parameters for the formation of the activated complex, they differ in the parameters for the conversion to the final complex ($-\Delta H_D^‡$, $T\Delta S_D^‡$). For WGA there is a further entropic barrier of 4 kcal mol^{-1} which is overcome by a large favorable enthalpy change, whereas for PNA the entropy change is slightly favorable (−2 kcal mol^{-1}) while the enthalpy decrease is somewhat smaller than for WGA. It is not possible to say at this time what the molecular bases of these differences might be in the transition from the immobilized activated complex to the final bound state.

Ionic forces are characterized by positive $\Delta S°$ values and small positive or negative $\Delta H°$'s [see Ross & Subramanian (1981)]. These types of electrostatic interactions are driven by the entropy gained upon binding which is in contrast to the results presented in this system. Therefore, ionic forces are not likely to be as important as hydrogen bonds and van der Walls' attractions in stabilizing this lectin–sugar complex. This is an important consideration in light of the belief that electrostatic forces between WGA, a basic protein, and acidic NeuNAc-containing molecules contribute to the association constant in solution to a significant degree (Monsigny et al., 1980). We would argue that these forces are minor in their contribution to the overall free energy of WGA–NeuNAc interactions.

The entropy barriers to binding imply that the dissociated state represents more disorder than do the transition or bound complexes. On binding, the loss of disorder offsets the energy gained by virtue of the hydrogen bonds and van der Waals' contacts achieved in the bound state. Thus, either or both of WGA I and N3L are more chaotropic when free in solution. We would suggest that the ligand, a polar molecule, is likely to disrupt the local water structure when free in solution. Upon binding, this chaotropic ability of the ligand would be lost by virtue of any hydrogen bonds that were now involved in the interaction with the protein site. This mechanism might account for the entropy barrier between the activated and final complexes, particularly if in the former the ligand is loosely associated with the protein but still partially solvated.

The existence of an entropic barrier to binding is irreconcilable with the model put forward by Kabat et al. (1981) to account for the "binding " specificity of several protein–sugar interactions that they studied. On the basis of the inhibition of agglutination results and the calculated preferred conformations of some of the ligands, they proposed that the hydrophobic effect was responsible for driving a hydrophobic patch of a ligand onto the hydrophobic surface of a protein. Such a model requires that the overall binding energetics be driven by a *positive* $\Delta S°$. The measured $\Delta S°$ values (Table IV) in this and other studies of lectin–sugar interactions are negative, the opposite to that required by the Kabat et al. (1981) model. Thus, the thermodynamic characterization (equilibrium and kinetic) of the two lectin–sugar complexes discussed above demonstrates that hydrogen bonding and van der Waals' forces are the most important factors in stabilizing the complex and not the hydrophobic effect.

It should be emphasized that the binding scheme presented in eq 2 and Figure 3 is the simplest consistent with the results obtained. More complicated reaction pathways can be envisaged that might also fit the data and that could perhaps be revealed by the application of other techniques. For example, Clegg et al. (1983) have interpreted temperature-jump experiments on the binding of MUF–$(GlcNAc)_n$ ligands to a mixture of WGA isolectins in terms of more complex binding mechanisms than that assumed above. Because a mixture of proteins was used and because of the inherent limitations in monitoring the environment of the fluorescent "tag" rather than the sugar moiety, we feel that their models are not applicable to our data.

WGA affinities for cell surfaces are found to be much greater than those for isolated oligosaccharides (J. P. Carver and P. M. Stanley, unpublished results). We have previously suggested (Kronis & Carver, 1982) that this might arise from simultaneous binding of a cell surface glycoprotein to both the S_{BC} and S_{AD} sites of WGA, thus leading to an overall free energy change twice that found for the isolated oligosaccharide. In agreement with that hypothesis, the results reported above suggest that a reduction in the entropy barrier(s) to binding at the cell surface could also lead to tighter binding. For example, one could envisage that $\Delta S_A^‡$ would be reduced for the occupation of other sites subsequent to the initial binding. This would arise since most of the rotational and translational degrees of freedom would have been lost in the formation of the initial complex. Another possible mechanism might arise if the solvation of the oligosaccharide portion of the cell surface

glycoprotein and/or glycolipid were significantly altered compared to that of an oligosaccharide free in solution. Clearly, further explorations of the peculiarities of the thermodynamics of protein–sugar binding at the cell surface are required.

ACKNOWLEDGMENTS

We express our gratitude to A. E. MacKenzie for helpful discussions and for providing his data on concanavalin A binding of glycopeptides and oligosaccharides prior to publication. We also thank B. D. Sykes for his comments on the binding model.

Registry No. N3L α2-3 isomer, 35890-38-1.

REFERENCES

Barker, R. (1971) *Organic Chemistry of Biological Compounds*, Prentice-Hall, Englewood Cliffs, NJ.
Clegg, R. M., Loontiens, F. G., Sharon, N., & Jovin, T. M. (1983) *Biochemistry 22*, 4797–4804.
Das, M. K., Zissis, E., & Glaudemans, C. P. J. (1979) *Carbohydr. Res. 73*, 235–244.
Edelman, G. M., & Wang, J. L. (1978) *J. Biol. Chem. 253*, 3016–3022.
Goldstein, I. J., Hughes, R. C., Monsigny, M., & Sharon, N. (1980) *Nature (London) 285*, 66.
Hardman, K. D., & Ainsworth, C. F. (1973) *Biochemistry 12*, 4442–4448.
Janin, J., & Chothia, C. (1978) *Biochemistry 17*, 2943–2947.
Kabat, E. A., Liao, J., Burzynska, M. H., Wong, T. C., Thorgersen, H., & Lemieux, R. U. (1981) *Mol. Immunol. 18*, 873–881.
Kronis, K. A. (1983) Ph.D. Thesis, University of Toronto, Toronto, Canada.
Kronis, K. A., & Carver, J. P. (1982) *Biochemistry 21*, 3050–3057.
Kronis, K. A., & Carver, J. P. (1985) *Biochemistry* (preceding paper in this issue).
Lacelle, N. (1979) Ph.D. Thesis, University of Toronto, Toronto.
Marchesi, V. T. (1972) *Methods Enzymol. 28*, 354–356.
Monsigny, M., Roche, A.-C., Sene, C., Maget-Dana, R., & Delmotte, F. (1980) *Eur. J. Biochem. 104*, 147–153.
Neurohr, K. J., Young, N. M., Smith, I. C. P., & Mantsch, H. H. (1981) *Biochemistry 20*, 3499–3504.
Neurohr, K. J., Mantsch, H. H., Young, N. M., & Bundle, D. R. (1982) *Biochemistry 21*, 498–503.
Privat, J.-P., Delmotte, F., Mialonier, G., Bouchard, P., & Monsigny, M. (1974) *Eur. J. Biochem. 47*, 5–14.
Rice, R. H., & Etzler, M. E. (1975) *Biochemistry 14*, 4093–4099.
Roberts, D. D., & Goldstein, I. J. (1982) *J. Biol. Chem. 257*, 11274–11277.
Ross, P. D., & Subramanian, S. (1981) *Biochemistry 20*, 3096–3102.
Swift, T. J., & Connick, R. E. (1962) *J. Chem. Phys. 37*, 307–320.
Van Landschoot, A., Loontiens, F. G., Clegg, R. M., Sharon, N., & De Bruyne, C. K. (1977) *Eur. J. Biochem. 79*, 275–283.
Wright, C. S. (1977) *J. Biol. 111*, 439–457.
Wright, C. S. (1980a) *J. Mol. Biol. 139*, 53–60.
Wright, C. S. (1980b) *J. Mol. Biol. 141*, 267–291.

Incorporation of 6-Carboxyfluorescein into Myosin Subfragment 1†

Dominique Mornet and Kathleen Ue*

Cardiovascular Research Institute, University of California, San Francisco, San Francisco, California 94143
Received May 31, 1984

ABSTRACT: We describe for the first time the introduction of a label into the "50K" domain of myosin subfragment 1 (S-1), and we investigate the properties of this fluorescent modification in relation to the ATPase and actin-binding activities, both residing in the myosin head. The labeling consists of a major incorporation of 6-carboxyfluorescein into the "50K" domain of S-1. Using different conditions for tryptic digestion that allowed a fragmentation of the "50K" domain with a loss of 5 kilodaltons (kDa) leading to a final product of 45 kDa, we have shown that the fluorescent dye remains in the 45-kDa final product. By studying cross-linking as a function of time, we have demonstrated that the "50K" domain and the 45-kDa fluorescent peptide are equally cross-linkable to actin. We have also investigated the K^+EDTA-, Ca^{2+}-, Mg^{2+}-, and actin-activated ATPase activities of this modified S-1 and after purification observed no enzymatic changes.

It was suggested early on (Kassab et al., 1981; Sutoh, 1982) that in the formation of the rigor complex there are contacts between actin and the "20K" region of myosin subfragment 1 (S-1)[1] and between actin and the "50K" region of S-1. This circumstance could arise if S-1 could bind simultaneously to two different actins, and indeed some structural reconstructions (Amos et al., 1982) have adopted this interpretation. However, the circumstance could also arise if, as suggested by Sutoh (1983) [see Heaphy & Tregear (1984) and Greene (1984) for recent confirmation], the same (one) actin can bind to the "20K" and "50K" regions. The electrophoretic band corre-

† This work was supported by Grant HL-16683 and a postdoctoral fellowship of the Muscular Dystrophy Association to D.M.

[1] Abbreviations: S-1, chymotryptic subfragment 1 of myosin; EDC, 1-ethyl-3-[3-(dimethylamino)propyl]carbodiimide; MES, 2-(*N*-morpholino)ethanesulfonic acid; TES, *N*-[tris(hydroxymethyl)methyl]-2-aminoethanesulfonic acid; ADP, adenosine 5′-diphosphate; ATP, adenosine 5′-triphosphate; kDa, kilodalton(s); EDTA, ethylenediaminetetraacetic acid; 1,5-IAEDANS, *N*-(iodoacetyl)-*N*′-(5-sulfo-1-naphthyl)ethylenediamine; PAGE, polyacrylamide gel electrophoresis; $NaDodSO_4$, sodium dodecyl sulfate; TPCK, L-1-(tosylamido)-2-phenylethyl chloromethyl ketone; Tris-HCl, tris(hydroxymethyl)aminomethane hydrochloride.

0006-2960/85/0424-0840$01.50/0